JOURNAL OF MAGNETIC RESONANCE 132, 65–77 (1998)
ARTICLE NO. MN981387

Uniform-Penalty Inversion of Multiexponential Decay Data

G. C. Borgia,* R. J. S. Brown,† and P. Fantazzini‡

*Department of ICMA, University of Bologna, Viale Risorgimento 2, 40136 Bologna, Italy; †515 W. 11th St., Claremont, California 91711-3721; and ‡Department of Physics, University of Bologna, Via Irnerio 46, 40126 Bologna, Italy

Received June 6, 1997; revised November 20, 1997

NMR relaxation data and those from many other physical measurements are sums of exponentially decaying components, combined with some unavoidable measurement noise. When decay data are inverted in order to give quasi-continuous distributions of relaxation times, some smoothing of the distributions is normally implemented to avoid excess variation. When the same distribution has a sharp peak and a much broader peak or a "tail," as for many porous media saturated with liquids, an inversion program using a fixed smoothing coefficient may broaden the sharp peak and/or break the wide peak or tail into several separate peaks, even if the coefficient is adaptively chosen in accord with the noise level of the data. We deal with this problem by using variable smoothing, determined by iterative feedback in such a way that the smoothing *penalty* is roughly constant. This uniform-penalty (UP) smoothing can give sharp lines, not broadened more than is consistent with the noise, and in the same distribution it can show a tail decades long without breaking it up into several peaks. The noise level must be known approximately, but it can be determined more than adequately by a preliminary inversion. The same iterative procedure is used to implement constraints such as non-negative (NN) or monotonic-from-peak (MT). The significance of an additional resolved peak may be tested by finding the cost of using MT to force a unimodal solution. A bimodal constraint can be applied. Decay data representing sharp lines in contact with broad features can require substantial computing time and some controls to stabilize the iterative sequence. However, UP can be made to function smoothly for a very wide variety of decay curves, which can be processed without adjustment of parameters, including the dimensionless smoothing parameters. Extensive testing has been done with artificial data. Examples are shown for artificial data, biological tissues, ceramic technology, and sandstones. Expressions are given relating noise level to line width and for significance of increase or decrease in error of fit. © 1998 Academic Press

INTRODUCTION

Nuclear magnetic relaxation data and many other kinds of physical data represent sums or distributions of decaying exponential functions. The decay curves and the corresponding distributions of exponential components vary greatly in character and complexity, but even the simplest relaxation data, with even a small amount of the unavoidable measurement noise, can be represented adequately by a wide variety of distributions of relaxation times. If no constraints are applied, such as smoothing or non-negativity, then these distributions are not even bounded.

Many authors have discussed the inversion problem (*1–12*) and given further references. Provencher (*1*) has provided an extensive discussion, and his CONTIN programs are widely used. Most inversion schemes apply both smoothing and other restrictions to prevent excessive detail in derived distributions of relaxation times. The non-negative (NN) constraint is usually applied on physical grounds, but it also serves to prevent wild oscillations in distributions, since an unnecessary but permissible high point is usually nearly canceled by a nearby negative point when NN is not applied. Another restriction is to limit the number of maxima to a small number such as one or two (*1*). This, too, can often eliminate spurious peaks and the undershoot that results from the smoothing of large narrow peaks. Of course, these restrictions may or may not be appropriate to the data. Most inversion processes minimize some function, usually mean-square, of the residuals plus some penalty function of the output distribution, together with constraints such as NN. A seldom used alternative is to impose minimum variation or variation-squared (*5*), subject to adequate fit to the data.

If the relaxation data have low noise level and are known from physical considerations to correspond to a small number of very well separated relaxation times, then even graphical peeling of longest components from semi-log plots can give times and amplitudes. Likewise, a nonlinear search by computer can give these components. However, if the components are not well separated, or if there is not valid *a priori* knowledge of the number of components, it is easy to misunderstand and misinterpret the computed results.

Another case is that of distributions with small numbers of well-separated peaks of finite width. Again, we may or may not have *a priori* reasons to know that a distribution is of this form. If the peaks are well separated, most inversion methods can give positions (relaxation times) and areas (corresponding signal amplitudes). If the peaks have similar widths on a logarithmic time scale, then most methods for inversion of relaxation data to get distributions of relaxation times will give also the correct peak widths if the data noise

1090-7807/98 $25.00

is sufficiently low and if the inverted data are smoothed to a degree appropriate to the noise level and peak width. If two peaks differ greatly in width, then it is not possible to choose a single smoothing parameter for the distribution that will not broaden the narrower peak and/or break the wider peak up into apparent multiple peaks.

The inversion problem is still more difficult when the resolution of peaks is marginal, especially when one peak is much larger than another. An especially difficult form of relaxation time distribution is found for fluids in complex porous media, such as brine in sandstone rocks, an important problem in the oil industry. A common form of distribution consists of a relatively high peak with a very long low tail extending to shorter relaxation times, often to times as short as a hundredth or a thousandth that of the peak. Such a tail, although very low, may have sufficient area to represent a substantial fraction of the initial signal (*13, 14*).

For several years we have dealt with this problem "manually" (*13*) by specifying widely different smoothing parameters for the relatively sharp peak and the long low tail. This procedure can also prevent the undershoot usually found at the sides of sharp peaks, which can give automatic minima between peaks and adjacent lower and broader features. The obvious drawback is that the choice of smoothing parameters is highly subjective. A welcome feature of the manually adjusted smoothing is that, with good data, the need for the application of a non-negative constraint may be greatly reduced or eliminated.

To reduce this subjectivity we have introduced negative feedback in the smoothing of the computed distributions of relaxation times to maintain roughly the same smoothing penalty for each computed point in a distribution. Instead of using a uniform smoothing *coefficient,* we vary the coefficient with relaxation time so as to keep the smoothing *penalty* roughly uniform. In this process the smoothing coefficient may vary by as much as nine decades, thereby avoiding the broadening of a very narrow peak and also avoiding breaking a wide feature into several apparent peaks. In the following we will first discuss the inversion problem and approaches to smoothing and then describe uniform-penalty (UP) smoothing.

INVERSION AND SMOOTHING

Relaxation Data

Most of our work with UP has been with longitudinal relaxation (T_1) data with random noise levels between 1% and 0.05% of the relaxing signal and with data (typically 127 points) taken at equal intervals in $q = \ln t$, where t is data time, usually over ranges of more than four decades. Data taken at equal intervals in q can best represent detail in different parts of wide distributions of relaxation times T, but transverse relaxation data (T_2), often by CPMG sequences, are inherently at equal intervals in t. These data can be inverted with UP smoothing also, but some additional bookkeeping is required.

We wish to compute a quasi-continuous distribution of relaxation times T in the form of a set of discrete points (usually from 80 to 110) covering about the same time range as the data and equally spaced in $Q = \ln T$. This gives spacings in q (data points) and Q (computed points) of the order of 0.1 Np (Neper). As will be seen later, this spacing is comparable to the minimum measurable peak half-width for a noise level of 0.25% of the integrated signal from the peak. To permit focus on the use of UP we will discuss only good data sets in the above form, excluding data equally spaced in time and avoiding data that do not adequately cover the ranges of relaxation times.

Least-Squares Inversion with Smoothing

As we have said, many very different distributions of relaxation times T can give adequate fits to a set of good relaxation data. Very large amounts of detail can be introduced in a distribution while still giving a good fit to the data. In fact, by introducing a lot of spurious detail it is possible to cancel some of the random noise that is part of all instrumental data sets. We may choose among fits with different amounts or types of detail on the basis of *a priori* knowledge, but, in most cases, we should probably choose what is in some sense the minimum amount of detail *demanded* by the data.

We wish to approximate a set of relaxation data s_i, taken at times t_i equally spaced in $q_i = \ln t_i$, by a sum of M exponential components,

$$s_i \approx g_0 + \sum_{k=1}^{M} g_k \exp(-t_i/T_k) \equiv x_i, \qquad [1]$$

where T_k are the relaxation times equally spaced in $Q = \ln T$ and covering about the same range as t_i. The distribution of amplitudes at relaxation times T_k (on the logarithmic time scale) is g_k, and g_0, the value of the signal at infinite time, is also a regression parameter. The computed fit to the data is x_i, as shown in Eq. [1]. To avoid excessive detail a penalty function is added to the squared error of fit, and their sum is minimized. Common penalty functions are squares of amplitude, slope (first difference), or curvature (second difference). The function to be minimized is then of the form

$$\sum_{i=1}^{N} (g_0 + \sum_{k=1}^{M} g_k \exp(-t_i/T_k) - s_i)^2 + A \sum_{k=1}^{M} g_k^2 + D \sum_{k=1}^{M-1} (g_{k+1} - g_k)^2 + C \sum_{k=2}^{M-1} (g_{k-1} - 2g_k + g_{k+1})^2, \qquad [2]$$

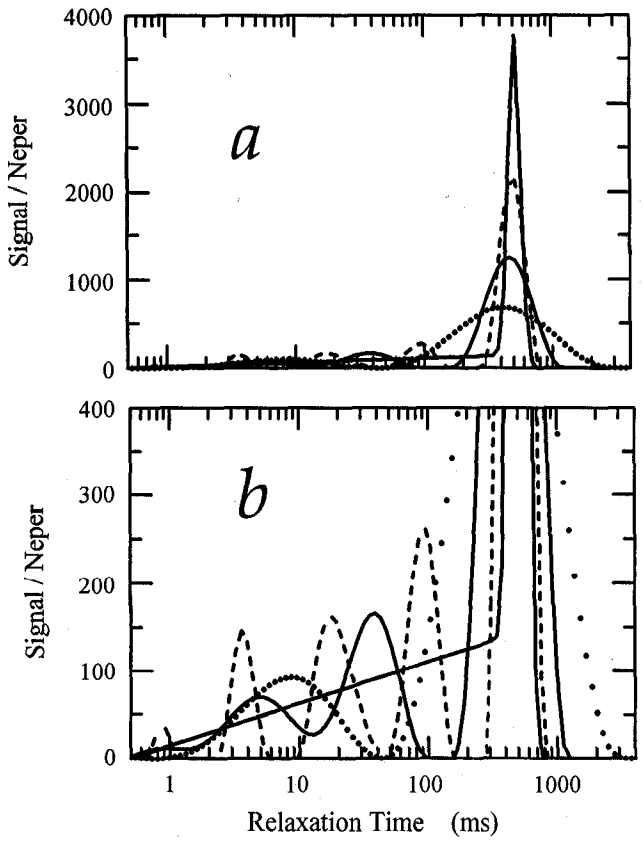

FIG. 1. Model distribution for artificial relaxation data and distributions computed with fixed smoothing parameters α (inversely proportional to the smoothing coefficients C). The artificial relaxation data are computed from the input distribution (model), which consists of a Gaussian line with integrated amplitude 1000, centered at 500 ms and with half-width (at $e^{-1/2} \times$ peak) 0.1 Np (Neper), plus a triangular tail with integrated amplitude 500 (representing an important one-third of the total initial signal) and tapering from the peak at 500 ms to zero at 0.5 ms. Pseudo-random noise with rms value 1.0 is added to the 127 artificial data points. The input model distribution is the higher solid curve in the full view (a) and the inner peak with triangular tail in the expanded view (b). The dashed curve in both views is for a constant smoothing parameter $\alpha = 10^8$. The lower solid curve in the full view (a), showing a wide peak and oscillatory tail in the expanded view (b), is for $\alpha = 10^5$. The remaining curve, shown by the unconnected computed points in both views, is for $\alpha = 100$. The inversion has 110 points spaced at $\approx$0.08 Np, and curvature smoothing is applied. The $\alpha = 10^8$ curve gives the correct noise value by slightly broadening the peak and thereby incurring a small penalty, which is made up by excessive detail on the tail, permitting the cancellation of some of the added noise. Note that each computed curve returns to the baseline to the left of the "real" peak, appearing to give one or more separate additional peaks. The non-negative (NN) constraint is applied to the computed curves.

where A is the coefficient for amplitude smoothing, D (difference) for slope smoothing, and C (curvature) for curvature smoothing (*1, 9, 10, 13*). We do not include the g_0 term in the penalty function. Usually only one of the three kinds of smoothing is used, and curvature smoothing is used in the present work.

Figure 1 shows the consequences of inversion with a fixed smoothing parameter C when a set of data has both sharp and broad features. Distributions of relaxation times are shown (as amount of initial signal per Neper of relaxation time) for different inversions of a single set of artificial data computed from a noise-free input distribution, or model, to which Gaussian random noise with unit rms amplitude has been added. In all cases the NN constraint, which often has a physical basis, is applied. The input distribution is a Gaussian peak with 0.1 Np half-width plus a triangular tail, contributing one-third of the initial signal and tapering to zero at short relaxation times. The smoothing effect of a given C value depends on the signal-to-noise ratio S/N and on the spacing of both the data points and the computed points. We will specify the degree of smoothing by a parameter α, which is inversely proportional to C (see later, below Eq. [9]) and has a smoothing effect that is not dependent (as for C) on the spacing of input data or of computed output points. To get from the minimization of Eq. [2] an adequate fit to the artificial data, represented in Fig. 1 and having known pseudo-random noise, it is necessary to use $\alpha = 10^8$. This still broadens the sharp peak somewhat, but it also breaks the tail into a number of separate peaks. In particular, it leaves a substantial interval of baseline between the real peak and the first spurious peak. The long tail needs many orders of magnitude more smoothing, and the transition needs to be abrupt. Even with $\alpha = 100$ the tail appears as a resolved separate peak, and the real peak is drastically broadened.

It may be noted that there are no spurious peaks to the right of the input peak. The NN constraint can prevent the undershoot, but the tail of the Gaussian is lost. NN also cancels zero-mean noise in the input time-domain data in relaxation-time regions of the computed fit amplitudes with little or no true signal; if the computed fit amplitude cannot go negative, it cannot go positive and retain the zero mean. To the left of the peak in Fig. 1, NN cannot prevent the undershoot and oscillatory behavior, because the output can go below its correct value without going negative.

In a sense, NN is overworked in many inversion procedures. When the expected distribution of relaxation times consists of one or several resolved peaks of different, but not drastically different, widths, it may be possible to choose an α that will not broaden the narrowest peak excessively and also not break a wider or lower peak into multiple peaks. In this case NN can prevent the undershoot at the sides of the peaks, sharpening the peaks and suppressing the noise. In this use NN serves more to stabilize a computation than to suppress measurable nonphysical features of the input data, such as effects of amplifier nonlinearity or drift. The results are often satisfactory when the conditions just mentioned are valid. However, there are many sources of relaxation data where the distributions of times do not consist of a few isolated peaks.

Relaxation data for visually homogeneous brine-saturated

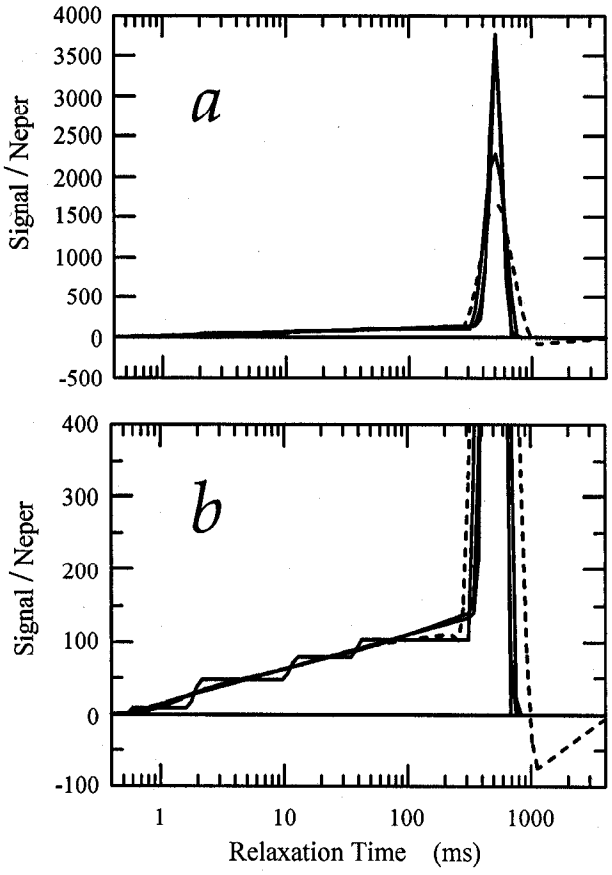

FIG. 2. Distributions computed from the same artificial relaxation data used in Fig. 1, with the model shown in both views as in Fig. 1. The lower solid curve in the full view (a), which has the stair-stepped tail in the expanded view (b), is computed with a fixed smoothing parameter $\alpha = 10^8$ and with the monotonic-from-peak (MT) constraint instead of NN. A third solid curve is shown in both views, which cannot be distinguished from the model on the scales shown here, for the distribution computed with uniform-penalty (UP) smoothing (to be described below) along with NN. The dashed curve in both views is for UP without either NN or MT. Here, the undershoot can be seen on both sides of the peak, and the peak is significantly broadened. However, most of the wild oscillation shown in Fig. 1 is avoided by the variable smoothing coefficient in UP.

oilfield rocks are often compatible with unimodal (with respect to $Q = \ln T$) distributions from one to three or more decades wide. There is a very wide variety of shapes, usually with more detail in one region than another. There exist examples with peaks with widths close to the minimum measurable values at their particular noise levels but with tails extending two or three decades. Thus, the artificial distribution of Fig. 1 is not unlike some found for fluids in the pores of rocks, although many rocks do not show peaks quite this sharp.

Distributions from the artificial data of Fig. 1 can be improved by applying a monotonic-from-peak (MT) constraint instead of NN, forcing the computed distribution to be unimodal. Although unimodal and bimodal constraints are mentioned as available in CONTIN (*1*), they appear not to be widely used for NMR relaxation data. The acceptability of the MT constraint *can be tested* by comparing the error of fit with MT against that with NN and applying resolution criteria, discussed later, to judge the significance of the extra cost of MT in error of fit.

Just as NN can *compensate* for undersmoothing on portions of distributions with noise but little or no signal, MT can *prevent* undersmoothing on broad features, whether with very little signal or with substantial signal. Of course, this is useful only if the cost is not enough to prevent an adequate fit to the data. Figure 2 shows the same artificial distribution as Fig. 1. The stairstepped curve is computed with a fixed $\alpha = 10^8$, using MT instead of NN. This gives a satisfactory distribution so long as one does not try to interpret the stairsteps. The use of MT prevents the extra peaks, but the triangular part of the distribution is still undersmoothed.

The application of UP smoothing, to be described in a later section, provides much stronger smoothing for the long tail than for the sharp peak. In Fig. 2, the computed distribution using UP and NN cannot easily be distinguished from the input distribution on the scales used in the figure. The computation using UP but not using either NN or MT (dashed lines) does show some undershoot on both sides of the peak, with some consequent broadening of the peak, but there is far less reliance on NN or MT than with fixed smoothing parameter.

INVERSION WITH VARIABLE SMOOTHING

To introduce more equitable smoothing for sharp and broad features we make A, D, and C in Eq. [2] variable, with subscript k, and move them inside the summations. Although variable smoothing can be implemented for amplitude, slope, or curvature smoothing, we will discuss only curvature smoothing, which we have used for a number of years. We have not tried the UP approach with amplitude or slope smoothing. The quantity to be minimized is now

$$\sum_{i=1}^{N} \left(g_0 + \sum_{k=1}^{M} g_k \exp(-t_i/T_k) - s_i\right)^2 + \sum_{k=2}^{M-1} C_k(g_{k-1} - 2g_k + g_{k+1})^2, \quad [3]$$

where C_k will be iteratively adjusted to be roughly reciprocal to the local curvature-squared (which itself depends on the C_k).

If the components g_k, s_i, and x_i make up the vectors **g** (computed distribution, $M + 1$ components), **s** (measured noisy signal, N components), and **x** (computed fit to the signal, N components), and if the components $\exp(-t_i/T_k)$ make up the $N \times (M + 1)$ matrix **U**, we have $\mathbf{x} = \mathbf{Ug}$. The

first term in Eq. [3] is then $\mathbf{g}^\dagger\mathbf{U}^\dagger\mathbf{U}\mathbf{g} - 2\mathbf{s}^\dagger\mathbf{U}\mathbf{g} + \mathbf{s}^\dagger\mathbf{s}$, with the last of these a constant. We let $\mathbf{U}^\dagger\mathbf{U} = \mathbf{W}$. This $(M + 1) \times (M + 1)$ matrix need be computed only once for the iterative computation of $\mathbf{g}$.

For the second (penalty) term in Eq. [3] we first find the contribution for unit C_k for a single k-value. This involves g_{k-1}, g_k, and g_{k+1}. The curvature (second difference) at the kth computed point is $\mathbf{V}^{(k)}\mathbf{g}$, where $\mathbf{V}^{(k)}$ is an $(M + 1) \times (M + 1)$ matrix containing all zero elements except for the submatrix

$$\begin{pmatrix} 0 & 0 & 0 \\ 1 & -2 & 1 \\ 0 & 0 & 0 \end{pmatrix} \qquad [4]$$

centered at the kth diagonal point. The contribution to the curvature-squared is $\mathbf{g}^\dagger\mathbf{V}^{(k)\dagger}\mathbf{V}^{(k)}\mathbf{g}$, where $\mathbf{V}^{(k)\dagger}\mathbf{V}^{(k)}$ is a symmetrical matrix containing all zero elements except for the submatrix

$$\begin{pmatrix} 1 & -2 & 1 \\ -2 & 4 & -2 \\ 1 & -2 & 1 \end{pmatrix}, \qquad [5]$$

centered at the kth diagonal element. We now form the matrix $\mathbf{K}$ (*Krümmung:* curvature) by multiplying each matrix $\mathbf{V}^{(k)\dagger}\mathbf{V}^{(k)}$ by C_k and summing the matrices for all k-values from 2 to $M - 1$. The total curvature penalty is $\mathbf{g}^\dagger\mathbf{K}\mathbf{g}$. Equation [3], and the quantity to be minimized, is now given by

$$\mathbf{g}^\dagger\mathbf{W}\mathbf{g} - 2\mathbf{s}^\dagger\mathbf{U}\mathbf{g} + \mathbf{s}^\dagger\mathbf{s} + \mathbf{g}^\dagger\mathbf{K}\mathbf{g}. \qquad [6]$$

We let $\mathbf{s}^\dagger\mathbf{U} = \mathbf{Y}$ and minimize the above expression by setting the gradient with respect to $\mathbf{g}$ to zero, giving

$$\mathbf{W}\mathbf{g} + \mathbf{K}\mathbf{g} = \mathbf{Y}; \quad \mathbf{g} = (\mathbf{W} + \mathbf{K})^{-1}\mathbf{Y}. \qquad [7]$$

FEEDBACK FOR UNIFORM PENALTY

Feedback

To have a strictly uniform penalty, that is, the same contribution to the right side of Eq. [3] for each value of k, we would have to find a way to make C_k inversely proportional to the square of the second difference. This can be done by a series of iterations, starting with a fixed C_k and for each new iteration letting C_k be inversely proportional to the square of the second difference from the previous iteration. This does give adequate fits to relaxation data, but it tends to give distributions consisting of straight-line segments, with too much detail in the form of abrupt bends. This can be improved considerably by relaxing the uniform-penalty requirement somewhat and using at each k the highest of the second-difference-squared values found at $k - 1$, k, or $k + 1$ from the previous iteration. That is, C_k for the next iteration is inversely proportional to the largest second-difference-squared found at k or a nearest neighbor. We can further improve appearance in many cases by using second-nearest neighbors or points from an even wider window. However, a wide window interferes with implementing abrupt changes in smoothing coefficient. It is also possible to use only slope-squared feedback (instead of curvature feedback) for curvature smoothing. In this case it is necessary to use the highest slope-squared over a window extending about 0.3 Np in relaxation time both above and below the point k. A useful compromise was found to be the use of both curvature and slope feedback, and for each k to use the highest values found at the point or a nearest neighbor.

The smoothing coefficients C_k are coefficients of rigidity for the computed distributions. Therefore, the feedback to adjust the C_k to give roughly uniform penalty consists of local *compliance* contributions from slope and curvature. We let c_k be the maximum value of $[(g_{l-1} - 2g_l + g_{l+1})/\Delta_Q^2]^2$ *for* $l = k - 1$, k, or $k + 1$. We likewise let p_k (*pendenza:* slope) be the maximum of $[(g_{l+1} - g_l)/\Delta_Q]^2$ for $l = k - 1$, k, or $k + 1$. The denominators, powers of the output interval Δ_Q in Q, make p_k and c_k discrete approximations to the squares of first and second derivatives of $g(Q)$ and hence as nearly as possible independent of Δ_Q. These parameters from one iteration are used to give the C_k's for the next.

Balance between Smoothing and Noise

The residuals term (left) and the penalty term (right) of Eq. [3] should somehow be balanced in finding the quantity to be minimized to get the distribution g_k. We still need global factors by which to multiply p_k and c_k to get C_k. We represent the compliance determined in one iteration in the form

$$\alpha_0 + \alpha_p p_k + \alpha_c c_k, \qquad [8]$$

where α_0, α_p, and α_c are constants that are not changed from one iteration to the next nor from one data set to the next. The term α_0 is a compliance floor, which should be small enough that it would never lead to undersmoothing, but which should be large enough to be a "seed" for the development of curvature in the iteration process.

For a good solution to good data the residuals term from the minimization of Eq. [3] is primarily due to the noise-squared. If R (*rumore, Rauschen:* noise) is the rms noise, the residuals term from Eq. [3] should be of the order of NR^2 if the fit is good. We assume that, in the vicinity of a solution, the two terms in Eq. [3] should be comparable. We need only proportionality, and we use proportionality to the density of points $1/\Delta_q$ instead of to N, having in mind

NOTE Subsequent tests show that the data point spacing Δ_q should not be *explicitly* related to the penalty, as it is in the paragraph before the one with Eq. [9]. Therefore, Δ_q^2 in Eq. [9] should be replaced by $0.08\,\Delta_q$, since we used Δ_q=0.08. No other result, computation, discussion, or conclusion is affected.

that data points well outside the range of relaxation times will not contribute much to *variability* in iterative approach to a solution. We could include R^2/Δ_q as a factor in C_k (and we would do this to deal with data equally spaced in time, where Δ_q is not constant). However, in our implementation we have instead normalized the input signal by dividing it by $R\sqrt{\Delta_q}$, and we have included a factor of Δ_q^{-2} in C_k to preserve the balance between noise and degree of smoothing. This makes the screen display during a computation proportional to an effective signal-to-noise ratio.

The amplitude is plotted as normalized signal per Np of $Q = \ln T$. To approximate an integral of the form $\int C(Q)(d^2g/dQ^2)^2 dQ$ for the curvature penalty by a discrete sum, we include a factor of the step size Δ_Q in the coefficient C_k. We now have

$$C_k = [\Delta_q^2 \Delta_Q^3(\alpha_0 + \alpha_p p_k + \alpha_c c_k)]^{-1}. \quad [9]$$

The symbol α (without subscript) will be used to indicate examples of fixed smoothing coefficient C, given in terms of $\alpha_0 = \alpha$ and $\alpha_p = \alpha_c = 0$ by Eq. [9].

CONSTRAINTS, CONVERGENCE, AND NOISE

Constraints: NN and MT

We use the same sequence of iterations to impose constraints, such as NN and MT. For each negative g_k in one iteration we impose NN by adding a large number to the kth diagonal element of $\mathbf{V}^{(k)\dagger}\mathbf{V}^{(k)}$ to force the corresponding g_k to be nearly zero in the next solution. By not forcing the point exactly to zero, we retain knowledge of its sign, which in some future iteration may cease to be negative, in which case the constraint for that point can be removed.

Likewise, we can reduce the slope for a pair of points nearly to zero by multiplying the submatrix (analogous to Eq. [5] for curvature),

$$\begin{pmatrix} 1 & -1 \\ -1 & 1 \end{pmatrix}, \quad [10]$$

by a large number and centering it between the diagonal elements k and $k + 1$ of $\mathbf{V}^{(k)\dagger}\mathbf{V}^{(k)}$. We can impose MT for sections of the computed distribution by reducing the slope nearly to zero when the slope is in the "wrong" direction. Again, we retain knowledge of the sign by not forcing the slope exactly to zero, and we can remove the constraint if it ceases to be needed.

We have also used a hybrid MT and NN constraint to allow a bimodal solution, where MT is applied before one peak and after the other, with NN applied between peaks. An example of this is shown later, in connection with Fig. 6. Another use of MT, not illustrated in this work, is to apply MT over short ranges of Δ_Q in order to remove unphysically sharp minima caused by undershoot.

In some cases we have tried to deal with nonideal data by imposing special constraints on the first and last points or the first and last several points, but, as we have said, the present discussion is focused on UP and is therefore limited to good data with random noise only and with adequate coverage of relaxation times.

Convergence

The iterative procedure for any combination of UP, NN, and MT does not necessarily converge. However, with reasonable parameters, it usually does converge for data sets not including overlapping broad features and sharp lines and for many data sets that do. With both sharp and broad features in contact it may take 30 or more iterations to settle to an approximate distribution with nearly constant error of fit, but it may never settle to one exact solution. To stabilize the iteration process at this stage (but not before), we use, for each k-value for the next iteration, the *smaller* of the newly computed C_k or the C_k that was used in the current iteration. It may be necessary also to suppress changes in the smoothing coefficients C_k when a large undershoot (negative point, to be suppressed in the next iteration) appears. This can break a nonproductive cycle of iterations. Also in such cases, it may be necessary to terminate iteration when the rms error of fit ceases to change significantly even if the changes in the C_k's do not converge to zero. These controls on the iterative process usually lead to a nearly steady state with substantially constant error of fit and without wandering appreciably from a region of nonconverging approximate solutions.

The computing time depends roughly on the cube of the number of computed points. Our computation is written in True Basic and run on a Pentium-90 computer, and we normally compute 110 points on a distribution of relaxation times, plus signal at infinite time. For each iteration it is necessary to invert a 111×111 matrix, which takes about 6 s. Each iteration takes about 12 s, so about 5 min is needed if 25 iterations are required. When very sharp features are absent, computing time is much less. It should be noted, however, that UP makes its greatest contribution when there are both broad and sharp features.

Coefficients, Artificial Data, and Noise

The coefficient α_0 in Eq. [9] should be chosen as large as possible without undersmoothing the widest distributions of interest. This is not critical. We have determined tentative values of α_p and α_c by setting one of them to zero and getting reasonable fits to artificial data with the other while using a window (see Feedback section) of ± 0.3 Np for determining maximum compliance (p_k or c_k) to use for a given k-value. Finally, we have made many computations with many forms

of artificial data to select the α's. Good results are obtained with $\alpha_0 = 1000$ (but smaller for very wide distributions with low S/N), $\alpha_p = 50$, and $\alpha_c = 10$. A wide variety of relaxation data can be inverted, giving the right scatter due to noise without changing the above α's.

We generate artificial data with pseudo-random noise, each noise point being obtained by subtracting 6 from the sum of 12 independent samples of pseudo-random numbers from a uniform distribution from 0 to 1, giving rms noise 1.0 and an approximately Gaussian distribution. In each case we record for reference the actual rms noise for the individual set of N artificial data points on a relaxation curve. We do not remove the mean, since our inversion computes the value for infinite time. Even for sets of $N = 127$ data points, there can be relative scatter (with respect to the ensemble mean value, N) of the sum of errors-squared of the order of $\sqrt{2/N}$, or 12.5% from data set to data set. This corresponds to a 6.3% variation in the rms noise for data sets of 127 points.

In processing an individual data set we deal with only one set of noise values, added to the signal values. Any fit to the noisy data set will make some accommodation to the noise, even if the fit is oversmoothed. Thus, adjusting smoothing parameters so that the rms residual is equal to the rms added noise results in slight oversmoothing, since some of the noise is still accommodated by the fit.

To adjust global smoothing parameters and to test UP we need to estimate the desirable level of the residual scatter for a fit. From artificial data, usually with 127 points, we have guessed an effective number of degrees of freedom, such as 7 (3 components: 3 amplitudes, 3 relaxation times, and signal at infinite time) to use with the number of data points and the known level of the added noise. For both artificial and natural data, we can get the residual scatter from a multicomponent discrete fit with up to 7 components (15 parameters) to the relaxation data. This has the advantage of having no smoothing parameters to choose. Additional components are computed until the best way to reduce the sum of residuals is to use a negative component or a component out of the range of the data times. An additional component is not used if its use does not reduce the standard deviation of the residuals. Agreement with the known noise of artificial data is very good.

We have two separate uses for a prior knowledge of the noise level. One is the normalization of the signal discussed just above Eq. [9]. This affects the smoothing in the computation, but it is not critical with respect to small changes, such as some tens percent. Even a factor of 2 is not drastic. If we have no prior knowledge of the noise level, a preliminary inversion would normally give a more than adequate value for the normalization. The other use for a prior knowledge of the noise is for selecting the α's. For this, we should know the noise level within from one to three percent for the ranges of parameters discussed here. However, after the α's have been selected by prior computation with artificial data, we do not need more than rough prior knowledge of the noise.

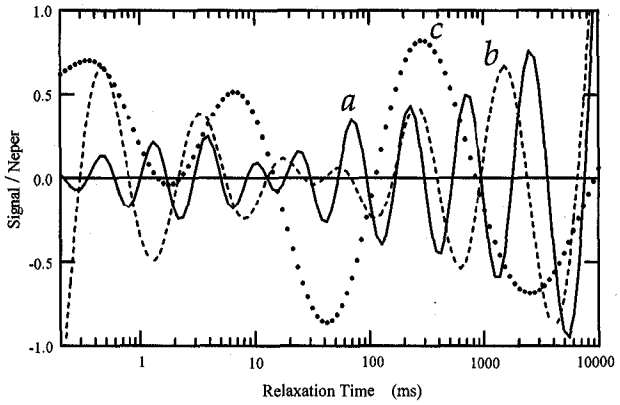

FIG. 3. Noise only, with unit rms amplitude, inverted without NN, MT, or UP (identified under Fig. 2). The solid curve (a) is for $\alpha = 10^{10}$ and is divided by 3400. The dashed curve (b) is for $\alpha = 10^6$ and is divided by 170. The curve with the unconnected dots (c) is for $\alpha = 10^2$ and is divided by 1.3. The smoothed fits reduce the input noise by 12.4%, 8.2%, and 4.1%, respectively. As α is increased (smoothing decreased) both amplitude and frequency of the excursions increase, and the rms scatter decreases. There is great variability from one set of noise values to another, but processing many sets of noise suggests that each cycle of the quasiperiodic oscillation tends to remove from the input noise about 2.2 degrees of freedom in addition to the two that would be removed by forcing the distribution to be a straight line.

The Noise by Itself

Figure 3 shows one sample of noise by itself inverted with fixed smoothing coefficient C and without NN, MT, or UP. Even a heavily smoothed fit removes some degrees of freedom and reduces the rms residual below the input noise. Clearly, the less the smoothing the more the fit can maneuver to accommodate the noise. The curve with the most oscillations (solid) reduces the noise by 12.4%, has $\alpha = \alpha_0 = 10^{10}$ (and $\alpha_p = \alpha_c = 0$), and is divided by 3400 for presentation on the scale shown. The dashed curve reduces noise by 8.2%, has $\alpha = 10^6$, and is divided by 170. The curve with the unconnected dots reduces noise by 4.1%, has $\alpha = 10^2$, and is divided by 1.3. The increase of amplitude and frequency of the excursions with decreased smoothing is accompanied by a decrease in the rms scatter. However, these features are highly variable from one set of noise values to another. Numerous sets of noise were processed with $\alpha = 10^m$ for integer m from 1 to 11, and cycles of quasi-periodic oscillation were counted (somewhat subjective). When the reduction of noise and cycles of oscillation were averaged for the sets of noise, a straight-line relationship (not shown) was found, suggesting that a cycle of oscillation tends to remove roughly 2.2 degrees of freedom in addition to the 2 that

would be removed by forcing the distribution to be a straight line with no oscillation at all.

RESOLUTION

Resolution of Two Lines

A rough criterion for the resolvability of two sharp lines can be inferred from Eq. [10] of Ref. (*15*) for the least maximum absolute error (LMAE) of fit to a rectangular distribution by two discrete exponential components. An approximate expression for the LMAE relative to initial signal, in terms of the line separation factor Y, is

$$E_2 = \frac{y^2}{6.87 + 15.9y + 7.2y^2}; \quad y = (\ln Y)^2/12. \quad [11]$$

Our ability to resolve the difference between the rectangular distribution and the two lines depends on our signal-to-noise ratio S/N and the density of data points in the region where the differences exist. Some rough simulations suggest that the effective region in signal time of significant signal differences corresponding to *localized* differences in distributions of relaxation times is of the order of a Neper. Thus, we have effectively $1/\Delta_q$ points helping statistically to determine the difference between models and reducing the required S/N by a factor of $\sqrt{\Delta_q}$. We then get a required S/N for resolution of two roughly equal lines,

$$S/N \gtrsim \sqrt{\Delta_q}/E_2. \quad [12]$$

For $Y = 3$ we get $E_2 = 0.0012$. If 127 data points extend in equal q-steps from 0.4 ms to 10 s, $\Delta_q = 0.080$, and $S/N \approx 240$ is a rough boundary for marginal resolution.

Figure 4 shows the UP-NN computations (with $\alpha_0 = 1000$, $\alpha_p = 50$, $\alpha_c = 10$) for four sets of artificial data with different selections of random noise with unit rms amplitude and with sharp lines for signal amplitude 100 each and a factor of 3 apart in relaxation time. Thus, $S/N = 200$, slightly less than the value 240 computed above for marginal resolution. We note that three of the four curves do not "resolve" the two lines. The curve with the two peaks does not have the lowest fit error relative to its added noise.

The above computations were repeated with $\alpha_c = 30$ instead of the "normal" 10. Here, each of the four curves gave two peaks. However, as before, the improvement in fit did not warrant the distinction between two peaks and a continuous distribution. The above were done also with additional sets of artificial data (not shown) with each peak of amplitude 250 instead of 100. In this case $S/N = 500$, which is well over 240, rather than slightly less. For these data the normal α's gave the two resolved peaks in all cases. Still another variation used pairs of identical Gaussian distributions meeting at two half-widths from their centers. The results (not shown) were substantially identical to those for the pairs of sharp lines.

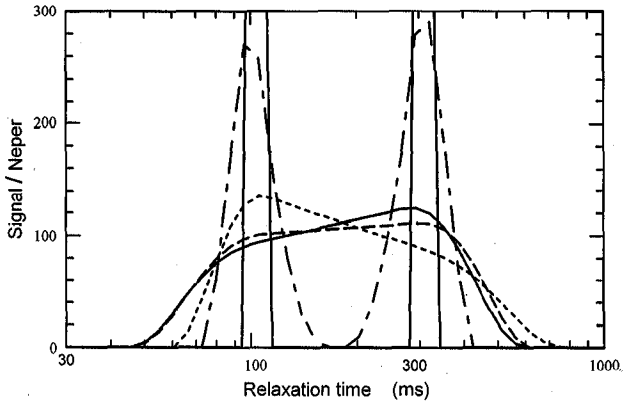

FIG. 4. Marginal resolution from artificial data for sharp lines at 104 ms and 310 ms, a factor of 3. Each of the two lines corresponds to a single exponential with initial signal = 100. The two peak positions are indicated by the two pairs of nearly vertical lines. Each of the four remaining curves shown is computed from a set of artificial data generated from the same model, but with an independent set of random noise values having unit rms amplitude. Inversions were made using UP-NN. One of the four curves (mixed dashes) breaks into two peaks at about the right positions, but the residual error of fit relative to the rms value of the its added random noise is not the lowest for the four curves. The other three (short-dashed curve, long-dashed curve, and on-scale solid curve) can be made to give two peaks by increasing the curvature-feedback compliance parameter from $\alpha_c = 10$ to $\alpha_c = 30$, but improvement in fit is not enough to give confidence that there are separate peaks. The two peaks are always resolved (with $\alpha_c = 10$) when each line amplitude is increased to 250 (not shown) instead of 100. The results were substantially the same for two Gaussian lines (not shown) meeting at two half-widths from their centers.

Linewidth Due to Noise

When noise is present, even a single-exponential signal can give a distribution with finite width. Equation [6] of Ref. (*15*) gives E_1, the LMAE for fit to a narrow rectangular distribution by a single line, analogous to Eq. [11] for two lines,

$$E_1 = 0.1086\, w^2, \quad [13]$$

where w is the half-width of the line in Np. In analogy with Eq. [12], we account for the density of data points by letting $S/N = \sqrt{\Delta_q}/E_1$, giving

$$w = 3.0\, \Delta_q^{1/4}/\sqrt{S/N}. \quad [14]$$

With $S/N = 100$ for a distribution consisting of a single line (as for each line of Fig. 4) and with the input data point spacing $\Delta_q = 0.080$ (127 points over a range of a factor of 25,000), $w = 0.16$ Np. Thus, the line half-width is about twice the output point spacing, $\Delta_q = 0.093$ (110 output points over a factor of 25,000). Increasing of S/N to 400

would give $w \approx \Delta_q$ for the above parameters. These values of w apply to isolated lines "protected" by either NN or MT, and the value of S/N applies to the line itself, not including other features of the distribution.

Significance Criteria for Improvement in Fit

As we have seen, it is possible to have quite different distributions adequately fitting a set of relaxation data. However, it is frequently useful to compare two or more solutions with differences due to the application of an additional constraint or of a change in a smoothing parameter, with the changes limited to a small range of relaxation times. It is not easy to decide by comparing fit errors alone whether one solution is significantly better than another. One problem is that a change primarily affecting one region, such as the foot of a peak, may also unintentionally and inconspicuously change the fit elsewhere, possible at very short times. However, we can estimate a minimum cost (*13, 15*) to warrant rejecting a restriction.

If a localized change in a distribution affects the corresponding decay curve over about a Neper, as discussed above, a change is not significant unless it affects the sum of errors-squared more than the probable effect of a different set of random noise values over this range. If there are enough points in this interval, the *variability* of the noise-squared is by a factor of about $\sqrt{2\Delta_q}$, where $1/\Delta_q$ is the number of points per Np. This factor times the number of points per Np is the variability, $\sqrt{2/\Delta_q}$, in the expected sum of noise-squared, N (with unit rms noise). This is a relative change of $\sqrt{2/\Delta_q}/N$ in the sum of errors-squared, giving a relative change in the rms fit error of half this amount,

$$1/(N\sqrt{2\Delta_q}). \qquad [15]$$

With $N = 127$ and $\Delta_q = 0.080$, Eq. [15] gives 2.0% as the relative increase in rms fit error for marginal significance of the extra cost of a constraint. This should be in addition to the cost of the roughly 2.2 fewer degrees of freedom for accommodating the noise if a cycle of oscillation is prevented by a constraint.

False Resolution from a Rectangular Distribution

The model for a set of artificial data is shown by the solid curve in Fig. 5. A rectangular distribution covers relaxation times over a factor of 7, with shape slightly affected by the necessary interpolation. As can be determined from Eq. [11] of Ref. (*15*), a rectangular distribution over a factor of 7 can be well approximated by two (not quite equal) lines spaced a factor of 3, as for the lines of Fig. 4. The integrated signal for the model is 200, and unit noise is added, as for Fig. 4. The line with the long dashes shows the UP-NN distribution computed with the normal parameters. The ends

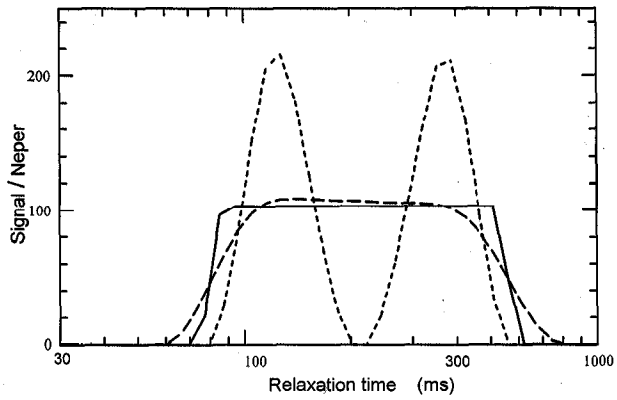

FIG. 5. Marginal false resolution from artificial data for a rectangular distribution. The solid curve is the input rectangular distribution (interpolated) with width a factor of 7, which can be well approximated by two (not precisely equal) lines a factor of 3 apart, as for the two lines of the model for Fig. 4. The area in the peak is 200, just as for the sum of the two lines of Fig. 4, and there is again unit rms noise. The curve with the long dashes is UP-NN with the curvature feedback parameter $\alpha_c = 10$ (normal), and the corresponding UP-MT (not shown) is substantially identical. The curve with two peaks, shown by the short dashes, is UP-NN with α_c increased to 30, the value that was required to get two separate peaks for all curves of Fig. 4.

are rounded, but the fit is good. If we increase α_c from 10 to 30, we resolve two false peaks, shown by the short-dashed curves, and improve the fit by 1% of the noise value. As mentioned before, this improvement is roughly equivalent to the removal of 2.2 degrees of freedom to accommodate noise by introducing a cycle of oscillation.

Resolution of Lines on a Pedestal

Although it was shown that UP can greatly decrease the reliance on NN, it does not by itself completely prevent undershoot and line broadening in the immediate vicinity of a sharp feature in a distribution. The resolution criterion of Eqs. [11], [12] does not apply unless we know that the choice is between either two sharp lines by themselves or else a compact distribution, such as rectangular or Gaussian, by itself. The solid curves in Fig. 6 show the input distribution for a pair of sharp lines a factor of 3 apart and on a wide pedestal. The short-dashed curve in the lower view is UP-NN for lines in the model with amplitudes 250 each and with unit noise. The mixed-dash curve is the same for amplitudes 500 each (and with a different noise vector, again with unit rms amplitude). In each case there is substantial undershoot below the pedestal, and the lines are not resolved. The undershoot is greater for the larger amplitude. If we increase the amplitude further, so that the undershoot is intercepted by NN (not shown), then the lines become resolved.

The unconnected plus signs (+) are for UP-MT, which avoids the undershoot but which, by its nature, does not permit two peaks. The upper view shows the input distribu-

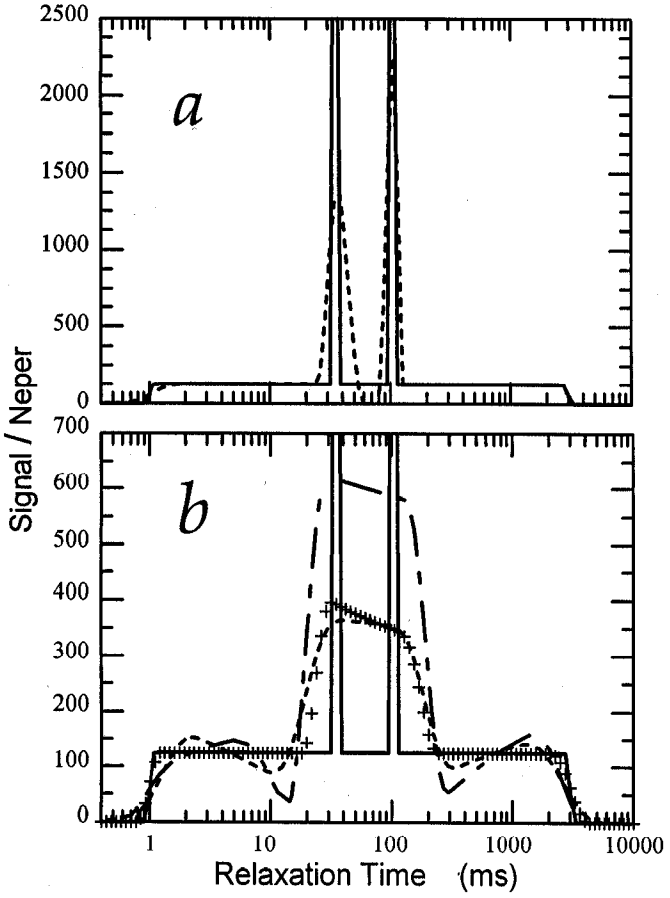

FIG. 6. Nonresolution of two single-line peaks, a factor of 3 apart, on a pedestal. Artificial data were generated for a model in which the area of the pedestal is 1000, that of each peak is 250, and unit rms noise is added. Without the pedestal these peaks are easily resolved by UP-NN with normal parameters. The solid curve is the input distribution in both displays. The short-dashed curve in the lower display (b) is computed by UP-NN. The unconnected plus signs (+) in (b) are for UP-MT for the same data. By its nature, MT cannot resolve the two peaks, but it does prevent the undershoot at the sides of the wide computed peak. The mixed-dash curve in the lower display is UP-NN for a model with the same pedestal but with each peak having area 500 instead of 250 and with a different selection of random noise, still with unit amplitude. The two peaks are still not resolved. If the signal is increased (with noise constant) until the undershoot goes negative and is intercepted by NN, then the peaks become resolved (not shown). The upper view (a) shows the input distribution (solid curve), and the dashed line is UP with a hybrid MT-NN, in which MT is applied before the first and after the second peak, while NN is applied between peaks. This bimodal constraint restores resolution of the lines.

tion (solid) and a UP solution with hybrid MT-NN constraints, where MT is applied before the first peak and after the second peak and where NN is applied between peaks. The peaks are now resolved and narrow, much as they are in the absence of the pedestal. The hybrid MT-NN constraint supplies information to permit identification of the sharp peaks much as NN does in the absence of the pedestal. In this example these constraints are appropriate, but they may or may not be appropriate for a data set for an unknown sample. In the latter case we may be able to judge the appropriateness of these constraints by the cost in terms of fit error.

Areas of Overlapping Peaks and of Undershoot

When, with UP-NN processing with normal parameters, two peaks appear separated by either a deep valley or a few points of baseline, it is clear that the phenomenon of undershoot has enhanced the valley or even brought the distribution down to the baseline for the few points. As computations with artificial data for pairs of Gaussian distribution with various combinations of heights, widths, and separations have shown, a few points of baseline in a computed distribution do not mean that the "real" peaks do not overlap. However, when the peaks are more than marginally resolved, according to the criterion of excess cost of the MT constraint, the areas of the peaks, as shown on cumulative distributions, are about right even when there is considerable disparity between the peaks. As always, the accuracy for a very small peak is limited. When UP is run without NN or MT on isolated peaks (or with NN for a peak on a pedestal, as discussed just above) the integrated area of the undershoot is usually between 1% and 5% that of the peak. This appears to be about the same for any value of S/N that permits a sharp peak. However, this percentage varies *erratically* with changes in Δ_Q or positions of the output points and with independent samples of the noise.

EXAMPLES

Biological Tissues

Figure 7 shows relaxation curves for a tumor-free portion of a length of human intestine resected because of cancer (*16*). The solid curve is for UP-NN, showing a peak with half-width 0.21 Np (measured at $e^{-1/2}$ height of peak) and with a tail representing about 24% of the signal. The long-dashed curve is with fixed $\alpha = 10^6$ with NN. The half-width of the peak is doubled, and a single satellite peak is shown representing 14% of the signal. The rms error of fit is 3.1% higher than for UP-NN, an amount which is slightly larger than the rough 2.0% found above to be marginally significant. The curve with the unconnected plotted points is also for fixed $\alpha = 10^6$ but with MT instead of NN, and the cost of eliminating the extra peak is about 0.3%, which is insignificant.

The short-dashed curve in Fig. 7 is for fixed $\alpha = 10^7$ with NN and shows two satellite peaks. The error of fit is 0.4% higher (insignificant) than for UP-NN, and the half-width is 1.8× that of UP-NN. This appears to be an example of the case where a fixed smoothing parameter oversmoothes a narrow peak and undersmoothes a broader feature, whether the "real" feature is a tail or a smaller and wider additional

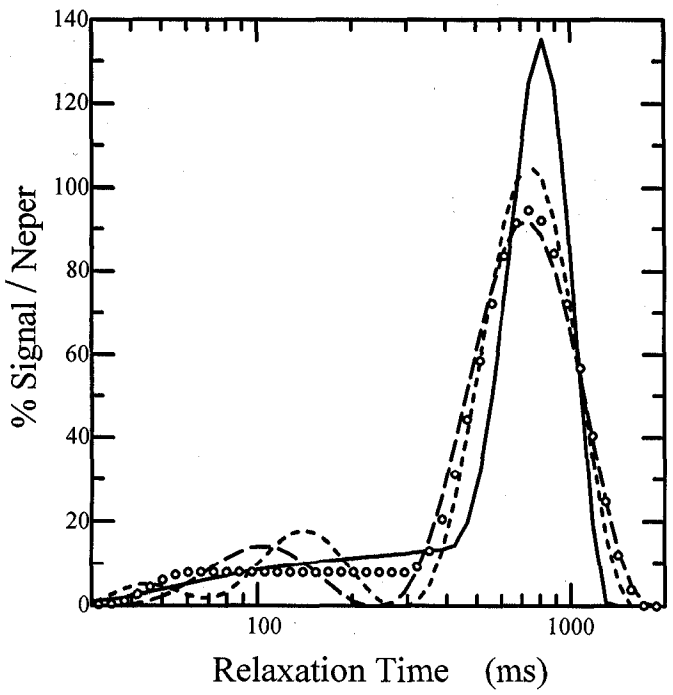

FIG. 7. Tissue from human intestine. The sample is a noncancerous piece of tissue from a length of intestine resected because of cancer. The solid curve is by UP-NN and consists of a peak and a tail. The short-dashed line, with two satellite peaks, is computed with constant $\alpha = 10^7$ and NN, with rms error of fit an insignificant 0.4% higher. The long-dashed curve, with the single satellite peak, is for fixed $\alpha = 10^6$ and NN. The rms error of fit is 3.1% more than for UP-NN, slightly over the approximate 2.0% for marginal significance. The unconnected plotted points are for $\alpha = 10^6$ with MT, and the cost of this constraint is insignificant. These relaxation data cannot by themselves tell us whether the tail is connected to the main peak or is one or more separate populations clearly separated in relaxation time from the peak. UP appears to give the least division into separate populations consistent with the data.

peak. The fixed smoothing parameter is a compromise between those needed for the two features, incurring a penalty for widening the peak and compensating for this by the oscillations in the broader feature, as discussed in connection with Fig. 3. The larger satellite peak represents 13% of the signal, and the smaller represents about 3.5%, with a sum of 16.5% of the signal separate from the main peak. It may be that broadening the peak (with respect to UP-NN) results in the inclusion of several percent of the tail (or second peak) in the main peak.

It should be emphasized that this set of relaxation data cannot by itself provide a firm choice between a tail and a second peak. If we have additional information, or if we make the hypothesis, that the distribution consists of a compact peak *without any tail* plus a wider additional peak, we can make an interpretation from any of the above displays. However, accuracy is limited, as the above different values of fractions of the total signal outside the main peak suggest.

Ceramic Technology

Figure 8 shows distributions of relaxation times computed by UP-NN for ceramic samples which had been fired at 950°C (a), 1000°C (b), 1050°C (c), 1100°C (d), and 1150°C (e); cooled; and saturated with water (*17*). The progression is to longer relaxation times with higher temperatures. At the lowest temperature the peak extends to 10 ms or slightly less. At higher temperatures, except for the highest, a tail still extends to a little below 10 ms, with the tails becoming smaller with increasing temperature. The UP-NN processing preserves even the very small tails without breaking them up into separate peaks. For these samples we have no *a priori* reason to expect separate peaks. At higher firing temperatures pores become larger and surfaces become smoother, leading to decreased surface-to-volume ratio and giving the longer relaxation times observed. As temperature is increased, sintering appears to eliminate the very small pores that contribute to the tail.

Porous Oilfield Sandstones

Figure 9 shows distributions of relaxation times for four oilfield sandstone samples which are relatively free of clay minerals and which are saturated with brine. These samples appear homogeneous to the eye, and porosities range from 3% to 16%. Each of the four distributions has significant contributions to the signal for relaxation times ranging over a factor of 1000. Each of the four distributions fits the data with rms scatter within about 1% that of the discrete multiexponential fits discussed under *Coefficients, Artificial Data, and Noise.* This guarantees that the peaks have not been broadened by oversmoothing for the two distributions that have peaks, and it can be seen that all the curves are smooth

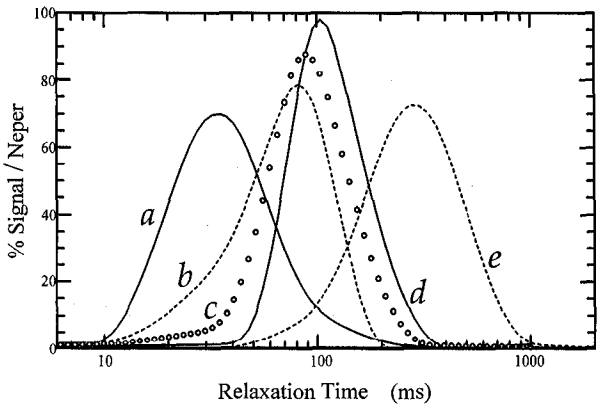

FIG. 8. Ceramic samples fired at different temperatures. Samples of the starting material for ceramics (so-called "green bodies") were fired, cooled, and saturated with water. Then T_1 relaxation data were taken, and distributions of relaxation times were computed by UP-NN and shown for the sequence of temperatures, 950°C (a), 1000°C (b), 1050°C (c), 1100°C (d), and 1150°C (e). Note the progressive loss with increased firing temperature of the tails at short relaxation times.

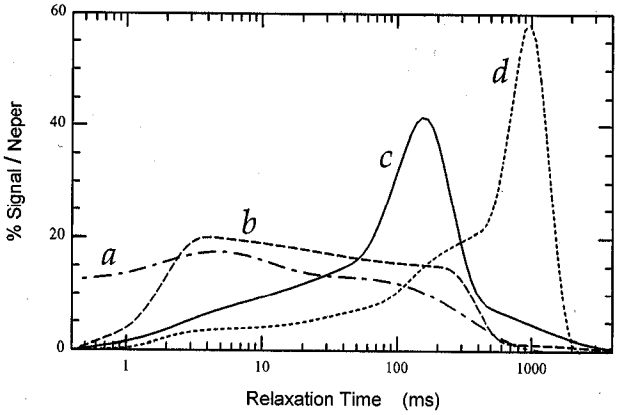

FIG. 9. Distributions computed using UP-NN from experimental NMR T_1 relaxation data for four visually homogeneous oilfield sandstone samples saturated with brine. The four samples were chosen all to have wide ranges of relaxation times but to exhibit quite different relaxation time distributions. Sample (a) has only 3% porosity and less than 0.1 mD permeability to fluid flow. (A Darcy is about a $(\mu m)^2$ and is a fairly large permeability for oil production; a mD is a small value.) Curves (b), (c), and (d) all have porosities in the 13–16% range. Permeability is not known for (b); it is 14 mD for (c) and 860 mD for (d). Long relaxation times correlate with high permeabilities. Note that all these curves are unimodal, as are most, but not all, distributions we have produced for brine-saturated sandstones that are visually homogeneous.

and unimodal. The good fit shows that additional detail is not *needed* for these data sets. It does not show that more complex solutions are wrong, and it does not show that data for the same samples taken with higher S/N or with the averaging of many signals could not require more detail.

Figure 10 shows computed distributions for a brine-saturated sandstone sample that has either a satellite peak or a knee several times as broad as the main peak and representing of the order of 20% of the initial signal. In turn, a tail or else still broader peak, representing about 10% of the signal, extends to still shorter times. The inset figure shows the region of the main peak. The diagonal squares are for the UP-NN computation, and the dashed line without plotted points is for UP-MT. The cost of the MT constraint was 2.4% of the rms noise level, which is marginal for resolving a separate peak from the main peak.

A solution (not shown) with UP and with MT before the middle peak and after the highest peak, and with NN between the two highest peaks, costs only 0.5% over UP-NN in additional scatter. Thus, the cost of preventing a minimum between the two smallest peaks is not even close to significant.

Rough simulations were made by means of three Gaussians as identified in the caption for Fig. 10. The same model was used with four selections of random noise. The distributions computed by UP-NN from the four sets of artificial data are shown by solid lines without plotted points. Two of these curves have substantial minima between the two smallest peaks, and the same two have greatly reduced separation between the two largest peaks. The width of the largest peak is substantially reduced for these two distributions, as can be seen in the inset figure showing the various representations of the largest peak. Cumulative distributions (not shown) for the computed distributions for the artificial data give the signals corresponding to the large peak (71%) to within 3.5% of the total signal.

As always, there is the possibility that one might have information in addition to that from the relaxation curve. For instance, if one knew *a priori* that the measured relaxation curve represented the sum of three Gaussian distributions, the amplitudes and widths could be estimated reasonably well from the relaxation data. However, in the case of the sandstone sample for Fig. 10, we do not have any convincing basis for a two- or three-compartment model, Gaussian or otherwise.

DISCUSSION AND CONCLUSIONS

The basic objective of UP inversion of relaxation curves is to give appropriate amounts of detail to both sharp and broad features, even when they appear on the same distribution of relaxation times. We have used an iterative procedure to imple-

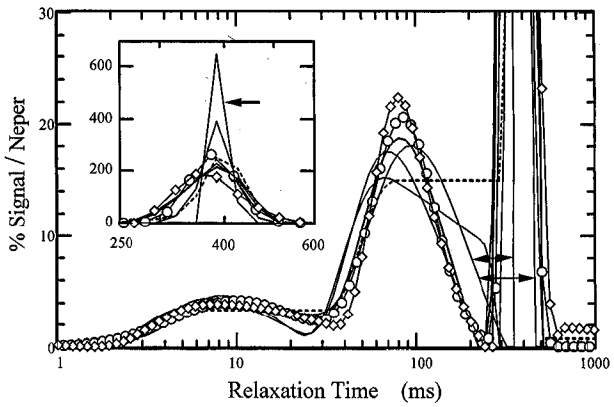

FIG. 10. Marginal resolution of a satellite peak (or shoulder) for an oilfield sandstone saturated with brine. The diagonal squares are computed by using UP-NN with the experimental relaxation data for the sandstone, and the dashed curve without plotted points is computed by using UP-MT. The cost of the MT constraint is 2.4% of the noise level, which, for the parameters involved, is marginal for identifying a resolved peak rather than a knee on the higher peak. The circles represent an input model for simulation of the computed distribution. The model consists of three Gaussians: 8.3% at 10 ms with half-width 0.8 Np, 20.6% at 85 ms with half-width 0.4 Np, and 71.1% at 380 ms with half-width 0.1 Np. The S/N is 1000 for the sandstone data and for the artificial data. Distributions computed by UP-NN are shown by solid lines without plotted points for four sets of artificial data, all for the above model but with different selections of random noise having the same rms value. In both the main figure and the inset, the arrows identify the one of these four distributions having the sharpest main peak, which is sharper than that of the model for the artificial data and sharper than that computed from the experimental data. It is illustrated that different selections of random noise can lead to strikingly different computed distributions and that noise can narrow a line as well as broaden it.

ment variable smoothing of the computed distributions, so that the smoothing *penalty* is roughly uniform over the sharp and broad features. This permits the computation of sharp lines without broadening by oversmoothing, and, in the same distribution, a broad feature can be smoothed sufficiently that it is not broken into unnecessary separate peaks.

There can be different objectives in the interpretation of distributions of exponentials. One important objective can be to know whether relaxation data (whether NMR or other) can reliably separate the source of signal into two or more populations. Examples could be oil and water in a porous rock, water in macropores and micropores in a rock having grains with internal porosity, tissue reached and not reached by contrast agent in biological systems, etc. Obviously, the existence of separate physical populations in a sample does not guarantee different or nonoverlapping relaxation times. In any case, there are important interpretation objectives where we wish to know if relaxation data *require* a significantly bimodal or multimodal distribution of relaxation times, suggesting separate populations. The UP inversion appears to suppress maxima and minima not required by the data, minimizing the appearance of separate populations in the computed distributions to the extent permitted by the data.

In many applications it may not affect interpretation if one peak is broadened somewhat to avoid breaking up a wider one. However, for many research applications it can be of interest to know the widths or shapes of lines, including when two or more lines of different widths are present, or when features with tails are present, and UP appears to give improved detail in these cases.

Constraints can be applied in the iterative procedure for UP, including the usual NN constraint. The MT constraint can force a unimodal solution. Hybrid constraints can allow a bimodal solution. Expressions are given relating noise level to linewidth for narrow lines, and expressions are given for significance of increase or decrease of error of fit when constraints are applied or altered. The cost of the MT constraint can indicate cases where the relaxation data require a multimodal solution.

The artificial data used in this work are well behaved in the sense that the sets of relaxation data are sums of positive exponential components with zero-mean Gaussian random noise added. The laboratory relaxation data appear to be well behaved in the same sense; the residual errors of fit appear random and independent of data time (inversion-recovery time for the experimental examples used). We have processed data sent by a correspondent, where instrumental problems have distorted relaxation curves. Here, inversions using NN give substantial sequences of residuals with the same sign. When UP without NN is applied to these data, very large positive and negative peaks are obtained. This gives evidence that the data are not a good set representing multiexponential decay with positive coefficients. As seen in Fig. 2, only slight undershoot is obtained with UP without NN for that set of good data. When one set of bad data was processed by UP-NN, two spurious sharp lines were produced, but the nonrandom residuals gave adequate warning, and UP without NN gave very large negative peaks and positive peaks.

In some combinations of sharp and broad features UP may require many iterations, and termination criteria other than convergence to infinitesimal differences between solutions may be necessary. Computing time can be substantial in the above circumstances, especially when output points more closely spaced than customary are used, as is useful to show the maximum amount of valid detail. However, these are just the circumstances where the variable smoothing feature of UP is most useful. With a few controls applied to the iterative cycle, UP has functioned well, without manipulation of parameters, on a very large variety of measured and artificial data.

ACKNOWLEDGMENTS

Investigation supported by University of Bologna (funds for selected research topics) and by Murst Grants.

REFERENCES

1. S. W. Provencher, *Comput. Phys. Comm.* **27** 213, 229 (1982).
2. J. P. Butler, J. A. Reeds, and S. V. Dawson, *SIAM J. Num. Anal.* **18,** 381 (1981).
3. M. G. Prammer, *in* "Soc. Petr. Eng. Ann. Tech Conf.," New Orleans SPE 28368, (1994).
4. R. Freedman, *in* "Soc. Petr. Eng. Ann. Tech Conf.," New Orleans, SPE 30560 (1994).
5. K. P. Whitall and A. L. Mackay, *J. Magn. Reson.* **84,** 134 (1989).
6. R. M. Kroeker and R. M. Henkelman, *J. Magn. Reson.* **69,** 218 (1986).
7. K. P. Whittall, M. J. Bronskill, and R. M. Henkelman, *J. Magn. Reson.* **95,** 221 (1991).
8. D. P. Gallegos and D. P. Smith, *J. Colloid Interface Sci.* **122,** 143 (1988).
9. H.-K. Liaw, R. Kulkarni, S. Chen, and A. T. Watson, *Am. Inst. Chem. Eng. J.* **42,** 538 (1996).
10. K.-J. Dunn, G. A. LaTorraca, J. L. Warner, and D. J. Bergman, *in* "Soc. Petr. Eng. Ann. Tech Conf.," New Orleans, SPE 28367 (1994).
11. K. P. Whittall, A. L. MacKay, D. A. Graeb, R. A. Nugent, D. K. B. Li, and D. W. Paty, *Magn. Reson. Med.* **37,** 34 (1997).
12. S. J. Graham, P. L. Stanchev, and M. J. Bronskill, *Magn. Reson. Med.* **35,** 370 (1996).
13. R. J. S. Brown, G. C. Borgia, P. Fantazzini, and E. Mesini, *Magn. Reson. Imag.* **9,** 687 (1991).
14. L. L. Latour, R. L. Kleinberg, P. P. Mitra, and C. H. Sotak, *J. Magn. Reson. Ser. A* **112,** 83 (1995).
15. R. J. S. Brown, *J. Magn. Reson.* **82,** 221 (1989).
16. P. Fantazzini and A. Sarra, *MAGMA* **4,** 1 (1996).
17. G. C. Borgia, P. Fantazzini, C. Palmonari, and G. Timellini, *Magn. Reson. Imaging* **14,** 899 (1996).